

## Photon Emission Spectroscopy of Individual Oxide-Supported Silver Clusters in a Scanning Tunneling Microscope

N. Nilus,\* N. Ernst, and H.-J. Freund

*Fritz-Haber Institut der Max-Planck-Gesellschaft, Faradayweg 4-6, D-14195 Berlin, Germany*

(Received 13 December 1999)

Photon emission spectra of individual alumina-supported silver clusters have been measured for the first time. The light emission stimulated by electron injection from the tip of a scanning tunneling microscope can be assigned to the (1,0) mode of the Mie-plasmon resonance in small silver particles. As cluster sizes decrease, the resonance position shifts to higher energies and the linewidth increases. In the size range examined (1.5–12 nm), intrinsic size effects are discussed as possible origins for the observed size dependence of the Mie resonance.

PACS numbers: 78.66.Vs, 36.40.Gk, 36.40.Vz, 61.16.Ch

Conventional electron and optical spectroscopies usually applied in surface science average over macroscopic areas of the sample. The experimental results are therefore obtained for an ensemble of objects inhomogeneously broadened by a number of statistical factors (size distribution of deposited particles, variations in the local environment). The structural and electronic properties of individual objects under study are often hidden in the ensemble average. Many attempts have been undertaken to increase the spatial resolution of the spectroscopy and to open up the possibility of investigating single, selected structures on a nanometer scale. Most of these experiments are based on the high resolution abilities of scanning tunneling microscopy (STM) and its variants. Tunneling spectroscopy allows the determination of the electronic structure of small metal clusters [1,2] and recently the observation of vibrational spectra of single adsorbed molecules [3]. Photon emission from the tunnel junction of an STM stimulated by inelastic tunneling processes can be used to measure the optical properties of the sample surface in the nanometer regime [4]. The method has been employed to record photon maps of semiconductors or metal films [5], nanocrystals [6,7], and individual molecules [8]. The spectroscopic mode allows the observed photon emission to be assigned to elementary processes such as interface plasmons in the tip-sample cavity or interband transitions in the sample [5].

Because of their characteristic surface plasmon resonance, silver particles have always played an outstanding role in absorption and emission spectroscopy [9]. The resonance position can be used to probe the size, shape, and chemical environment of the clusters. A large number of measurements are available for ensembles of silver particles which are either supported on insulating surfaces (quartz [10],  $\text{TiO}_2$  [11]) or embedded in weakly interacting matrices (glass [12], argon [13]). Various theoretical models have been developed to explain the experimental data [13–15]. In this paper we report photon emission spectra of individual oxide-supported Ag clusters as a function of size. The clusters were deposited on a thin, well-ordered alumina film, suitable for the application of STM. We present the energetic position of the Mie resonances for

cluster sizes between 1.5–12 nm diameter as well as the width of resonances for individual clusters.

In the experiment, photon emission of supported silver clusters was stimulated by the field emission current of an STM, using the tip as the local electron emitter. Benefiting from the open construction and the large acceptance angle for the light collection, a beetle-type STM surrounded by a parabolic mirror was used. The STM setup is mounted in a UHV chamber (pressure:  $p = 2 \times 10^{-10}$  mbar) equipped with the standard techniques for sample preparation and analysis. Outside the vacuum chamber the light was focused onto the slit of a UV/visible-grating spectrograph and detected with a liquid nitrogen cooled CCD camera. Silver was evaporated from a crucible by electron bombardment and deposited at 300 K onto a thin, well-ordered alumina film grown on a NiAl(110) surface [16]. Because of a weak metal-oxide interaction, silver grows at 300 K in the Volmer-Weber mode forming 3D particles [17]. Step edges and domain boundaries of the alumina film are the preferential nucleation centers [Fig. 1(a)]. Additional nucleation centers due to the impact of  $\text{Ag}^+$  ions are formed when the sample is kept at a negative potential relative to the evaporator [Fig. 1(b)]. This procedure leads to a stable surface morphology. Modifications of the clusters

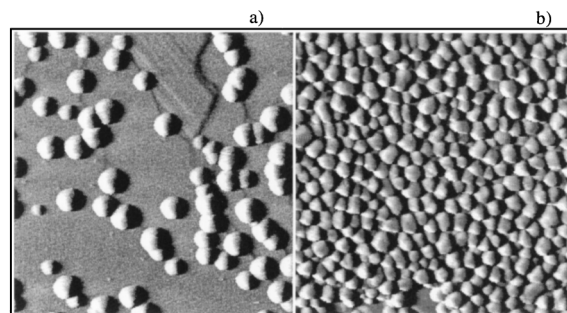


FIG. 1. STM images of Ag clusters on  $\text{Al}_2\text{O}_3/\text{NiAl}(110)$  grown by vapor deposition (image sizes:  $130 \text{ nm} \times 130 \text{ nm}$ ,  $U_{\text{tip}} = -2 \text{ V}$ ,  $I_{\text{gap}} = 0.6 \text{ nA}$ ). The sample was held at 0 V (a) and  $-500 \text{ V}$  (b) relative to the evaporator during Ag deposition. Only clusters in (b) were stable enough to be analyzed.

during the spectroscopic run were excluded with an STM image taken after each measurement. Depending on the amount of evaporated material the mean cluster size can be adjusted between 1–12 nm. Cluster diameters have been obtained after separating the effect of tip convolution. This was achieved by extracting a mean tip radius from the apparent broadening of substrate step edges. However, the given sizes still represent an upper limit of the real cluster diameter. Photon emission spectra of the clean alumina film on NiAl(110) are governed by two resonances of a tip induced plasmon at 1.3 and 2.4 eV excited in the NiAl/W tunnel junction [18]. This interface plasmon is the result of a strong electromagnetic interaction between tip and sample causing collective electronic oscillations in the coupled electron gases [19]. The emitted light intensity vanishes at a tip bias above 10 V reflecting the retraction of the tip and the reduced electromagnetic coupling between tip and sample at higher voltages.

Spectra taken on top of an Ag cluster exhibit an intense emission line, centered around 3.7 eV (Fig. 2). The light intensity increases for tip voltages above 10 V and is polarity dependent, visible only for electron injection into the cluster. This behavior cannot be understood using the concept of a radiating decay of the Ag/W interface plasmon, which is polarity independent by definition. Comparing the energetic position of the observed line with published experimental data suggests an assignment to Mie resonances inside the Ag cluster [9]. These resonances can be interpreted as collective oscillations of the free cluster electrons with respect to the Ag-ion cores driven by an external electromagnetic field (UV radiation) or electron injection. For nonspherical, supported metal clusters, the Mie resonance splits into two modes corresponding to an electron oscillation parallel (1,1 mode) and perpendicular (1,0 mode) to the substrate [9]. Only for the (1,0) mode, a dipole excitation process of the plasmon is efficient because the electron injection from the tip follows the surface normal and induces a dipole perpendicular to the surface

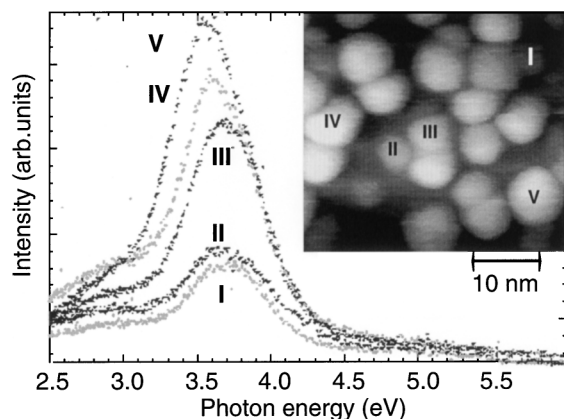


FIG. 2. Photon emission spectra of differently sized Ag clusters (accumulation time 500 s,  $U_{\text{tip}} = -10$  V,  $I_{\text{gap}} = 10$  nA). The inset shows the corresponding STM image.

plane. Also, an electron impact excitation preferentially transfers a momentum perpendicular to the surface. On the other side, a Mie plasmon oscillating in the surface plane will be quenched by its image dipole induced in the NiAl(110) substrate. Therefore, the single emission line visible in the spectra has to be attributed to the decay of the (1,0) Mie resonance in the Ag cluster. The lateral resolution of the photon emission spectroscopy is determined by the diameter of the exciting electron beam. For a tip voltage of 10 V and an electron current of 10 nA used in the experiments, the mean tip-sample separation can be estimated as 1.0–1.5 nm, depending on the tip radius. The excitation of optical processes is therefore restricted to a sample area smaller than 1.5 nm in diameter, and the emission has to be assigned to an individual Ag cluster. The measured peak position, full width at half maximum (FWHM) and intensity of the emission line can be evaluated as a function of size and shape of a single cluster.

The intensity variation of the emission for differently sized Ag particles can clearly be distinguished in the data shown in Fig. 2. The emitted total light intensity increases with cluster size, reflecting the growing number of electrons participating in the plasmon oscillation. The peak positions move to higher photon energies (blueshift) with decreasing cluster sizes. The low total photon yield emitted from an individual Ag cluster complicates the evaluation of the FWHM of the Mie resonance. The linewidths measured in Fig. 2 result from a compromise between a reasonable signal-to-noise ratio and an optimal spectral resolution determined by the size of the entrance slit of the spectrograph. For the experimental data shown, a slit width of 1 mm was used and the FWHM of the resonance is additionally broadened by the transfer function of the spectrograph. For a slit width below 0.2 mm, the experimental broadening of the emission line is negligible, but the required accumulation time has to be extended. The increase of the homogeneous linewidth for decreasing cluster sizes is plotted in Fig. 3 (slit width

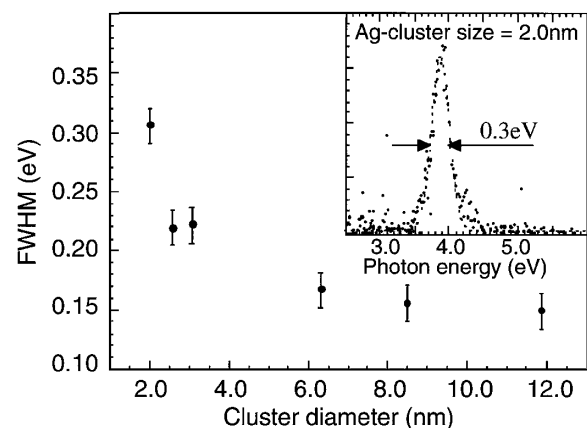


FIG. 3. FWHM of the Mie resonance as a function of the cluster diameter. The inset shows a photon emission spectrum measured with high spectral resolution (slit width: 0.2 mm).

0.2 nm). The behavior reflects the reduced lifetime of a collective oscillation in small particles due to the enhanced surface scattering rate. This additional decay mechanism (apart from electron-electron and electron-phonon scattering) becomes highly efficient when the electron mean path exceeds the cluster diameter [9]. The determination of the linewidth for a single particle allows an estimate of inhomogeneous line broadening effects due to the size distribution of particles in an ensemble. We note that a minimum linewidth of 230 meV has previously been obtained for an ensemble of quartz-supported Ag clusters with 10 nm mean diameter and a narrow size distribution ( $\sigma = 0.13$ ) [20]. The difference to our result (150 meV for clusters of 10 nm) shows the effect of inhomogeneous line broadening.

Figure 4 demonstrates the shift of the resonance position to higher energies as the cluster diameter decreases. This size dependence is in contrast to extinction cross section measurements performed on an ensemble of Ag clusters deposited on quartz [10]. Here a distinct redshift of the (1, 0) mode with decreasing cluster size was observed. The result was interpreted as a consequence of a transition from oblate to spherical shapes for decreasing cluster diameter. For electro-dynamical reasons this increase of the axial ratio (cluster height/diameter) causes a redshift of the (1, 0) mode and a blueshift of the (1, 1) mode. In the present experiments, a shape dependence of the resonance position can be ruled out. A careful determination of the cluster shapes from STM images leads to an almost constant axial ratio of  $(0.59 \pm 0.10)$  in the size range examined. Only particles in the upper size regime generally grow in a more oblate shape with an axial ratio slightly below 0.5.

Neglecting the shape dependence, we will concentrate on intrinsic size effects as the reason for the observed blueshift of the Mie resonance. Intrinsic size effects (e.g., spillout of the Ag 5s electrons, hybridization of Ag 5s and 4d electrons) have the general trend of following a  $1/d$  law ( $d$  cluster diameter), reflecting the growing surface contribution with respect to bulk effects in small particles

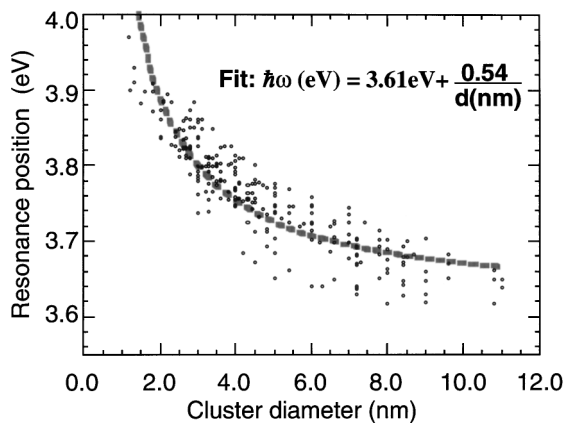


FIG. 4. Peak position of the Mie resonance as a function of cluster diameter.

[9,21]. A corresponding fit function of the type

$$\hbar\omega(d) = \hbar\omega(\infty) + \frac{a}{d} \quad (1)$$

already reveals a qualitative agreement with our experimental data (dashed line in Fig. 4). This  $1/d$  behavior further supports our interpretation that the blueshift is caused by intrinsic size effects. The above mentioned contributions to the size effect cannot be extracted from the experimental data, however, two results of the empirical description have to be emphasized. The value  $\hbar\omega(\infty)$  for large silver particles should be in agreement with the predictions of the classical Mie theory. A crude estimation of the resonance position can be derived from the following formula [22]:

$$\varepsilon_1(\omega) = -\varepsilon_m^* \frac{1 - L_\perp}{L_\perp}. \quad (2)$$

Here  $\varepsilon_m$  is the averaged static dielectric constant of the medium surrounding the cluster, consisting of 70% vacuum ( $\varepsilon_m = 1$ ) and 30% alumina film ( $\varepsilon_m = 3.13$  [23]), and  $L_\perp$  is the geometrical depolarization factor along the surface normal estimated to 0.4 for the given cluster shape. Values for the dielectric function of silver have been taken from the literature [24]. The calculated resonance position of 3.45 eV is significantly lower than the experimental value of 3.6 eV. Two reasons may be responsible for this difference. The Ag clusters are separated from the NiAl substrate by an alumina film of only 0.5 nm thickness. The presence of the metal causes a strong interaction between the electron oscillation in the cluster and its image dipole in the NiAl surface. Together with the general enhancement of the vertical component of the electromagnetic near field at a metal surface, this may explain a “stiffening” of the resonance and a blueshift of the plasmon frequency. Additionally, the internal plasmon potential is affected by the electrostatic field induced by the negatively charged tip. This additional field pushes the silver electrons at the exposed surface into the cluster volume and leads to a local increase of the electron density [25]. The consequence is a further shift of the resonance position to higher energies. However, cathodoluminescence measurements performed on a cluster ensemble of Ag/Al<sub>2</sub>O<sub>3</sub>/NiAl(110) in the absence of an electric field reveal almost the same value for  $\hbar\omega(\infty)$  [26]. A significant field-induced effect on the Mie-resonance position can therefore be excluded.

The factor  $a$  describing the size dependence of the resonance position was obtained as 0.54 eV nm from Eq. (1). For Ag clusters embedded in weakly interacting media or vacuum, this value is the result of two major competing processes [27,28]. A decrease of the cluster diameter leads to a growing fraction of electrons residing outside the classical cluster volume. This spillout effect reduces the density of the 5s electrons inside the cluster and lowers the plasma frequency of the electron gas. The spillout contribution causes a redshift of the Mie resonance in

small clusters and a negative  $a$  value. The size dependent screening efficiency of the Mie plasmon due to the Ag  $4d$  electrons leads to an opposite size effect in the resonance energy. The strong depolarization field of the  $d$  bands considerably lowers the plasma frequency of the free electron gas. The screening efficiency is reduced at the cluster surface, because the  $d$  electrons are stronger localized and cannot spill out into the vacuum thus far. The electron gas at the cluster surface is hardly affected by the depolarization field of the  $4d$  electrons and enhances its plasma frequency towards the unscreened value. The growing surface to volume ratio leads to an increase of the total Mie-plasmon energy in small Ag clusters and counteracts the spillout effect (high  $a$  value). Our experimentally determined blueshift of the resonance position for supported Ag clusters ( $a = 0.54$  eV nm) is considerably higher than for Ag clusters in vacuum ( $a = 0.18$  eV nm) [29]. This result seems to be reasonable because the efficiency of the spillout effect is strongly reduced at the cluster-alumina interface, and its contribution to the frequency shift should be less important compared to free particles. However, for Ag clusters enclosed in an argon matrix the spillout effect is suppressed at the whole cluster surface [30]. The hybridization effect dominates the size dependence of the Mie-resonance position, thus explaining the pronounced blueshift. As expected, the corresponding  $a$  factor of 0.8 eV nm for this system [13] clearly exceeds the value for the supported Ag clusters in the present experiment. These considerations give only qualitative arguments for an understanding of the observed dependence of the Mie resonance on the cluster size. A comprehensive explanation of the observed blueshift has to include a separate treatment of all competing processes contributing to the intrinsic size effect, especially the screening efficiency of the Ag  $4d$  electrons and the electron density variation at the cluster surface and the cluster-oxide interface.

In conclusion, we have reported photon emission spectroscopy of individual, oxide-supported silver clusters performed in an STM. The spectra are dominated by an intense emission line centered around 3.7 eV, which can be attributed to the (1, 0) mode of the Mie resonance in small silver particles. Peak position, FWHM, and intensity of the emission line could be determined for a single cluster. The observed blueshift of the resonance position with decreasing cluster size cannot be explained by a shape transition but reflects the growing importance of quantum size effects in the size range examined. The interplay between the electron spillout and the ( $s$ ,  $d$ )-electron hybridization effect in small Ag particles is discussed as a model to understand the observed size dependence of the Mie plasmon.

For financial support we are grateful to the Deutsche Forschungsgemeinschaft, the Fond der Chemischen Industrie, and the NEDO International Joint Research Grant on Photon and Electron Controlled Surface Processes.

\*Corresponding author.

Email address: nilius@fhi-berlin.mpg.de

- [1] A. Bettac, L. Köller, V. Rank, and K.H. Meiwes-Broer, *Surf. Sci.* **402**, 475 (1998).
- [2] J. Li, W.D. Schneider, R. Berndt, and S. Crampin, *Phys. Rev. Lett.* **80**, 3332 (1998).
- [3] B.C. Stipe, M. Rezaei, and W. Ho, *Science* **280**, 1732 (1998).
- [4] J.H. Coombs, J.K. Gimzewski, B. Reihl, J.K. Sass, and R.R. Schlittler, *J. Microsc.* **152**, 325 (1988).
- [5] R. Berndt, in *Scanning Probe Microscopy*, edited by R. Wiesendanger, Springer Series Nanoscience and Technology (Springer-Verlag, Berlin, 1998), p. 97.
- [6] A. Downes and M.E. Welland, *Appl. Phys. Lett.* **72**, 2671 (1998).
- [7] P. Dumas, C. Syrykh, I. Makarenko, and F. Salvan, *Europhys. Lett.* **40**, 447 (1997).
- [8] R. Berndt, R. Gaisch, J.K. Gimzewski, B. Reihl, R.R. Schlittler, W.D. Schneider, and M. Tschudy, *Science* **262**, 1425 (1993).
- [9] U. Kreibig and W. Vollmer, *Optical Properties of Metal Clusters*, Springer Series Materials Science Vol. 25 (Springer-Verlag, Berlin, 1995).
- [10] T. Wenzel, J. Bosbach, F. Stietz, and F. Träger, *Surf. Sci.* **432**, 257 (1999).
- [11] D. Martin, J. Jupille, and Y. Borensztein, *Surf. Sci.* **402**, 433 (1998).
- [12] U. Kreibig and L. Genzel, *Surf. Sci.* **156**, 678 (1985).
- [13] W. Ekardt, D.B. Tran Thoai, F. Frank, and W. Schulze, *Solid State Commun.* **46**, 571 (1983).
- [14] T. Yamaguchi, S. Yoshida, and A. Kinbara, *Thin Solid Films* **21**, 173 (1974).
- [15] I. Simonsen, R. Lazzari, J. Jupille, and S. Roux, *Phys. Rev. B* **61**, 7722 (2000).
- [16] R.M. Jaeger, H. Kuhlbeck, H.-J. Freund, M. Wuttig, W. Hoffmann, R. Franchy, and H. Ibach, *Surf. Sci.* **259**, 235 (1991).
- [17] M. Bäumer and H.-J. Freund, *Prog. Surf. Sci.* **61**, 127 (1999).
- [18] N. Nilus, N. Ernst, P. Johansson, and H.-J. Freund, *Phys. Rev. B* (to be published).
- [19] P. Johansson, R. Monreal, and P. Apell, *Phys. Rev. B* **42**, 9210 (1990).
- [20] F. Stietz and F. Träger, *Philos. Mag. B* **79**, 1281 (1999).
- [21] K.-P. Charlé, L. König, S. Nepijko, I. Rabin, and W. Schulze, *Cryst. Res. Technol.* **33**, 1085 (1998).
- [22] R. Gans, *Ann. Phys. (Leipzig)* **37**, 881 (1912).
- [23] *Metals: Electronic Transport Phenomena*, edited by K.-H. Hellwege and J. Olsen, Landolt-Börnstein, New Series, Group III, Vol. 15b (Springer-Verlag, Berlin/Heidelberg, 1985).
- [24] H. Ehrenreich and H. Philipp, *Phys. Rev.* **128**, 1622 (1962).
- [25] P. Gies and R. Gerhardt, *Phys. Rev. B* **33**, 982 (1986).
- [26] M. Adelt, W. Drachsel, and H.-J. Freund (unpublished).
- [27] W. Ekardt, W.-D. Schöne, and J. Pacheco, in *Metal Clusters*, edited by W. Ekardt (Wiley, New York, 1999), p. 1.
- [28] A. Liebsch, *Phys. Rev. B* **48**, 11317 (1993).
- [29] J. Tiggesbäumker, L. Köller, K.H. Meiwes-Broer, and A. Liebsch, *Phys. Rev. A* **48**, R17490 (1993).
- [30] A. Zangwill, *Physics at Surfaces* (Cambridge University Press, Cambridge, England, 1988), p. 200.